and 1.37 required to scale nitrate to ammonium and sodium nitrate, respectively. In addition, carbon was not apportioned between elemental and organic, and a single multiplier of 1.3 was used to give best agreement in regression of aggregated mass-closure mass on measured $PM_{10}$. Figure 6.34 shows the mean chemical apportionment for this site. The mean $PM_{10}$ was 18.9 µg $m^{-3}$ (gravimetric). Approximately one-third, on average – that is, ~7 µg $m^{-3}$ (gravimetric) – of $PM_{10}$ at this urban background site in Glasgow is constituted by primary mechanically (wind)-generated particles, that is, dust and sea salt. The relatively high proportion of sea salt is due to Glasgow's west coast location. Approximately one-third of the $PM_{10}$ is due to secondary inorganic aerosol. The remaining one-third is carbonaceous aerosol, although this cannot be apportioned between primary elemental carbon from local sources and organic carbon either from local sources or as longer range secondary organic aerosol.

**Figure 6.34** Apportionment of urban background $PM_{10}$ in Glasgow using the mass closure model of Harrison *et al*. (2003). Proportions are means of $n$ = 182 samples.

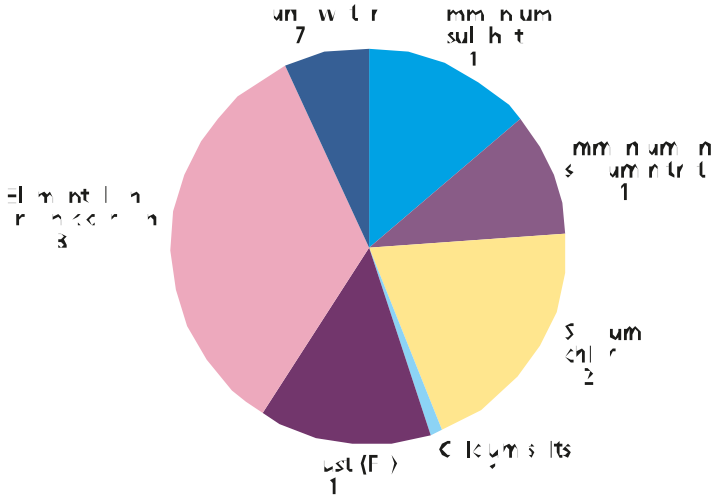

## 6.2 Spatial distribution of PM

### 6.2.1 Spatial distribution of $PM_{10}$ within and between Edinburgh and Glasgow

**557.** Measurements of daily $PM_{10}$ at two separate urban centre sites in Edinburgh and at two separate urban centre sites in Glasgow provide evidence of a reasonably strong spatial correlation in background $PM_{10}$ for both cities, see Figures 6.35 and 6.36 ($r$ = 0.64 and $r$ = 0.56 for Edinburgh and Glasgow, respectively).

**558.** The value of the correlation coefficient ($r$ = 0.50) between the mean of the $PM_{10}$ from the two sites in Edinburgh and the mean of the $PM_{10}$ from the two sites in Glasgow for almost 1 year's measurements is almost as strong as the correlation in $PM_{10}$ within each city (Figure 6.37). Although these two cities are separated by only ~80 km, these data indicate that for roughly comparable cities in the UK, a significant proportion of variability in $PM_{10}$ is controlled by regional-scale sources and synoptic meteorology.

**Figure 6.35** Correlation between daily $PM_{10}$ at two sites in Edinburgh (1999–2000).

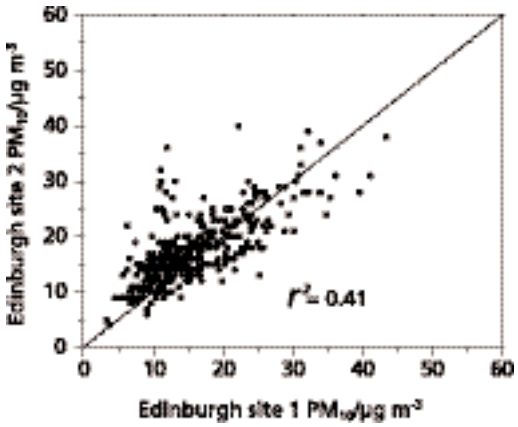


**Figure 6.36** Correlation between daily $PM_{10}$ at two sites in Glasgow (1999–2000).

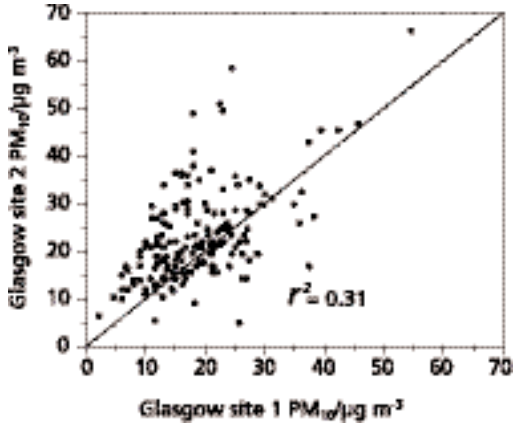


**Figure 6.37** Correlation between mean daily $PM_{10}$ at two sites in Edinburgh and two sites in Glasgow (1999–2000).

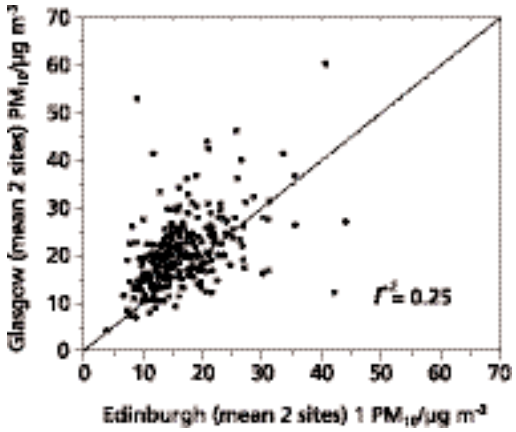


## 6.2.2 Regional distribution of $PM_{10}$ and $PM_{2.5}$ concentrations across London

**559.** An analysis of the frequency distribution of the hourly $PM_{10}$ concentrations observed at the London North Kensington site during 2002 (see Figure 6.38) reveals the presence of a long tail of hourly values that reach to levels that are over five-times the median concentration. In contrast, the frequency distribution shows that concentrations that are one-fifth of the median concentrations are relatively rare. A simple explanation of the relative absence of low concentrations would be that there is a background concentration below which hourly values are infrequent. Examination of the frequency distributions observed at other sites in the LAQN shows that this is a universal feature.

**560.** To understand better the nature of the background concentration observed in the frequency distribution at the London North Kensington site, a detailed analysis was made of the spatial distribution of the $PM_{10}$ observations compiled in the LAQN. Two transects, 20 km-wide, were constructed through the London conurbation in a north-south and a east-west direction, and the $PM_{10}$ concentrations were plotted for those sites that fell within the transects. Figure

**Figure 6.38** The frequency distribution of the hourly mean $PM_{10}$ concentrations observed during 2002 at the London North Kensington site.

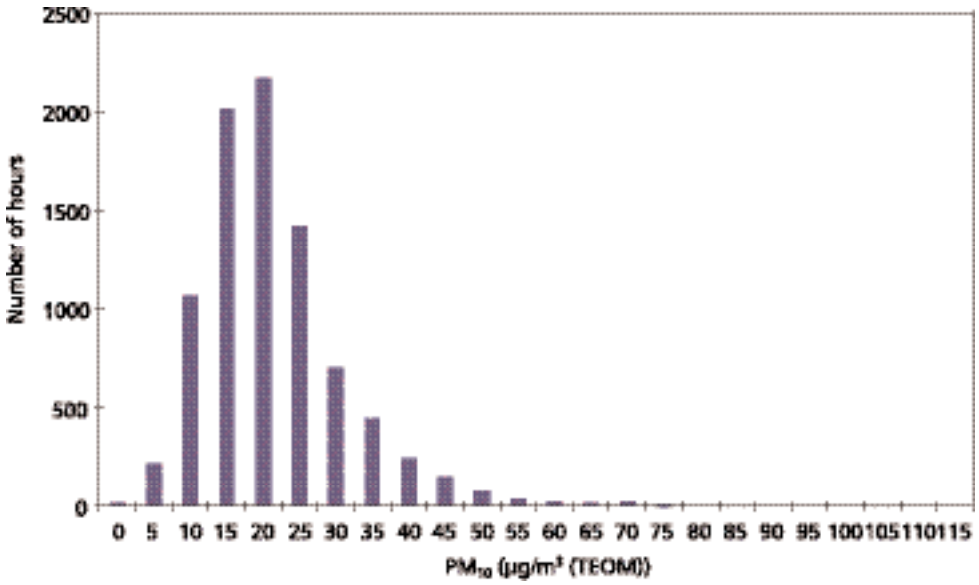


6.39 shows the distribution of $PM_{10}$ concentrations in the north-south transect and Figure 6.40 in the east-west transect. Each transect passed through central London and all data were the annual mean concentrations for 2002.

**561.** Broadly speaking, $PM_{10}$ levels rose towards the middle of each transect for both sites away from traffic and those influenced by traffic and fell off towards the ends of the transects. There is clear evidence within both these plots for a background concentration upon which the London contribution stands. In Figures 6.39 and 6.40, the presence of such a background is indicated by the straight line set at 16.5 µg $m^{-3}$.

**562.** The value of 16.5 µg $m^{-3}$ for the regional background across London was chosen as follows. From the LAQN, ten sites were selected that were located on the periphery of London and away from the immediate influence of traffic. The sites were: Crawley background, Dacorum background, East Hertfordshire background, Hertsmere background, Horsham background, Mole Valley 1, North Hertfordshire background, Sussex mobile, Luton background and Thanet Airport. The mean of the sites was calculated for each hour of 2002, and an hourly time series of background concentrations was constructed. The annual mean of this synthetic time series was 16.5 µg $m^{-3}$.

**563.** This background concentration was then subtracted from each hourly value for each site in the LAQN to obtain a time series of background-corrected values. The 47 sites that were sited away from traffic exhibited an average annual $PM_{10}$ concentration of 19.9 µg $m^{-3}$ and of 4.6 µg $m^{-3}$ when the hourly background concentrations were subtracted. The sites that were under the influence of traffic showed an average annual $PM_{10}$ concentration of 26.0 µg $m^{-3}$ and of 9.3 µg $m^{-3}$ when the background was subtracted. On this basis it appears that a substantial fraction of the observed $PM_{10}$ concentrations observed at sites within the LAQN can be attributed to the regional background and that a relatively smaller fraction was due to emissions within the London conurbation.

**Figure 6.39** Annual $PM_{10}$ concentrations for 2002 for those LAQN sites within a 20 km-wide transect that passes north-south through the London conurbation.

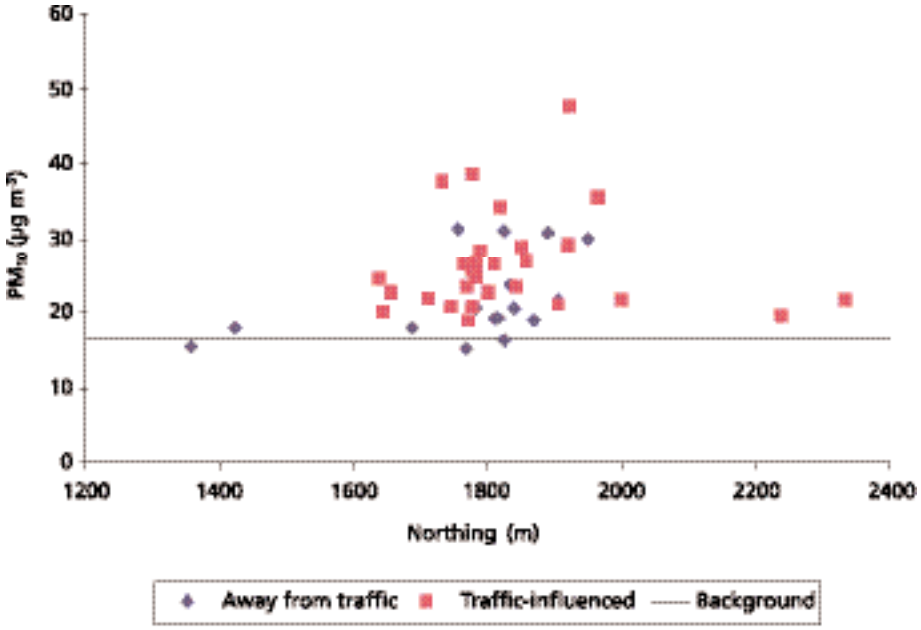


**Figure 6.40** Annual $PM_{10}$ concentrations for 2002 for those LAQN sites within a 20 km wide transect which passes east-west through the London conurbation.

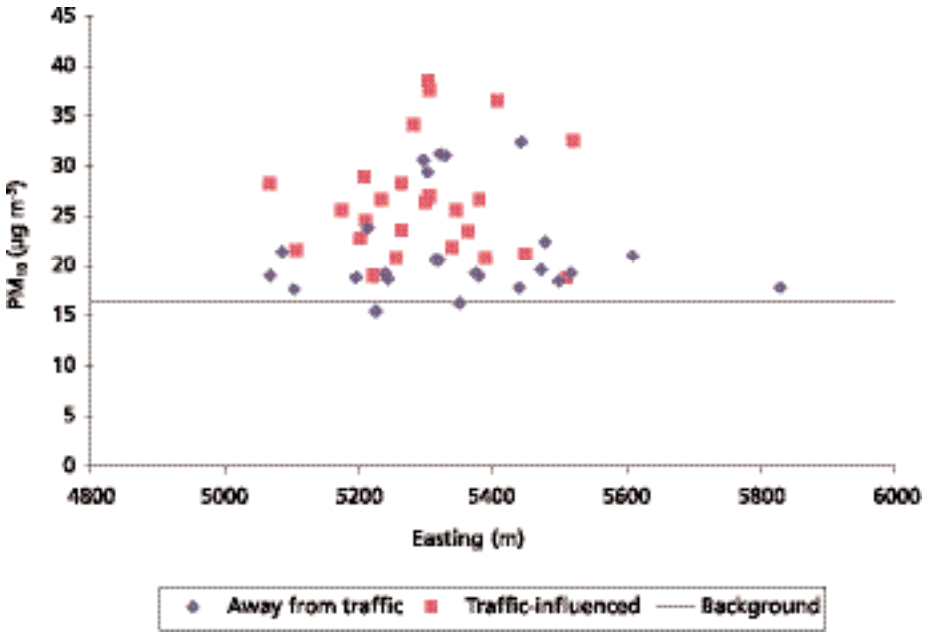


**564.** The corresponding analysis for $PM_{2.5}$ is hampered by the availability of $PM_{2.5}$ monitoring sites but the main principles still apply. The frequency distribution of the hourly $PM_{2.5}$ concentrations observed at the Ealing roadside site show the presence of a background below which observed concentrations are infrequent. Two sites were selected for the attribution of a background concentration for each hour of 2002 and this value was subtracted from each of the $PM_{2.5}$ observations at the LAQN sites. The background sites selected were the London Bexley and Rochester sites and an annual mean background concentration of 10.9 µg $m^{-3}$ was inferred. The annual mean of the four LAQN sites monitoring

$PM_{2.5}$ in 2002 was 15.2 µg $m^{-3}$, 3.9 µg $m^{-3}$ with the background subtracted. On this basis it was concluded that the regional background contributed a substantial fraction of the $PM_{2.5}$ concentrations observed across London.

### 6.2.3 Background concentration surfaces of $PM_{10}$ in London

**565.** The spatial distribution of city-scale background concentrations of $PM_{10}$ was assessed through interpolation of monitored data for selected sites in and around London. The use of monitoring data to investigate spatial patterns in concentrations is useful for complementing the more detailed spatial representations derived from air quality models. Interpolated maps of monitoring data tend to give a broad impression of the pattern of concentrations in a particular area. In this case, the maps estimate concentrations at background locations only. They do not include contributions from specific local sources, particularly roadside or kerbside locations, which would tend to increase concentrations from those shown in this section. Surfaces have been produced for annual average concentrations in 2003 and 2002 and for shorter averaging periods for two contrasting $PM_{10}$ episodes during February 2003 and August 2003.

#### *6.2.3.1 Annual mean background concentrations in London*

**566.** Interpolated surfaces were generated using ordinary kriging with 25 TEOM sites from the London and the Southeast networks. Sites were discarded from the analysis if they were classified as kerbside or roadside or if there was a data capture rate of less than 60%. Due to a relatively uneven spatial distribution of the location of urban background sites, it was necessary to include suburban and urban centre sites in the analysis (see Figure 6.41 and Table 6.10). Monitored annual means for 2003 ranged between 23–32 µg $m^{-3}$. The standard scaling factor of 1.3 was applied, but it is recognised that this may not adequately account for the true local geographic variability in concentrations (Green *et al.*, 2001).

**Figure 6.41** Locations and siting characteristics of monitoring sites used to estimate the spatial distribution of annual mean concentrations.

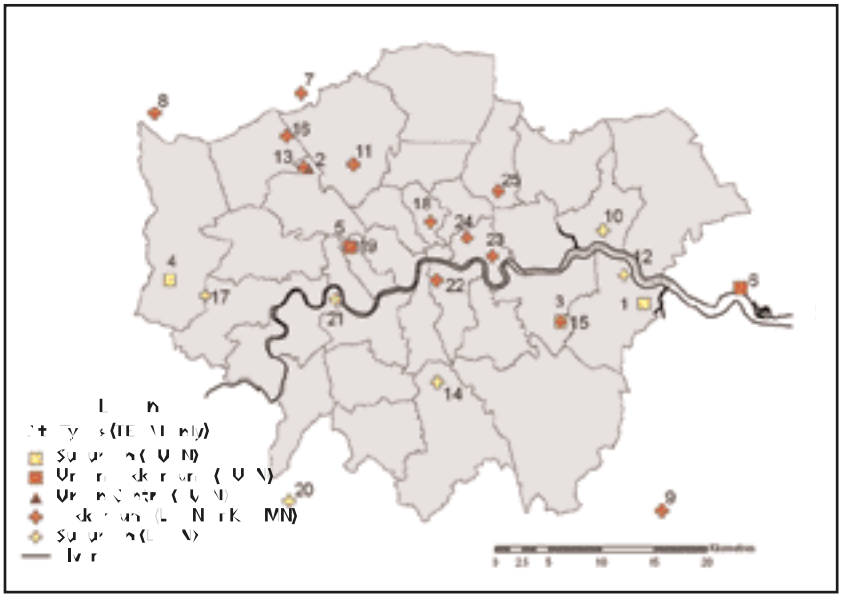

**Table 6.10** Summary of 2003 PM monitoring data from sites shown in Figure 6.47.

| Number | Name | Max daily mean TEOM* 1.3 (µg $m^{-3}$) | Date of max daily mean | Days >50 µg $m^{-3}$ | Data capture (%) | Annual mean TEOM* 1.3 (µg $m^{-3}$) |
|---|---|---|---|---|---|---|
| 1 | London Bexley | 79 | 26/03 | 33 | 87 | 27 |
| 2 | London Brent | 81 | 22/02 | 24 | 86 | 27 |
| 3 | London Eltham | 79 | 26/03 | 24 | 89 | 27 |
| 4 | London Hillingdon | 129 | 01/11 | 28 | 80 | 30 |
| 5 | London North Kensington | 77 | 08/08 | 28 | 88 | 29 |
| 6 | Thurrock | 135 | 09/04 | 38 | 88 | 31 |
| 7 | Hertsmere (Borehamwood) | 70 | 20/04 | 20 | 88 | 25 |
| 8 | Three rivers background | 75 | 22/02 | 27 | 78 | 23 |
| 9 | Sevenoaks 2 – Greatness | 77 | 29/03 | 14 | 91 | 23 |
| 10 | Barking and Dagenham 2 – Scrattons Farm | 78 | 20/03 | 43 | 89 | 32 |
| 11 | Barnet 2 – Finchley | 70 | 10/08 | 23 | 90 | 26 |
| 12 | Bexley 2 – Belvedere | 78 | 15/04 | 30 | 88 | 27 |
| 13 | Brent 1 – Kingsbury | 81 | 22/02 | 25 | 86 | 26 |
| 14 | Croydon 3 – Thornton Heath | 79 | 26/03 | 17 | 86 | 26 |
| 15 | Greenwich 4 – Eltham | 78 | 26/03 | 24 | 91 | 27 |
| 16 | Harrow 1 – Stanmore background | 72 | 11/08 | 16 | 85 | 23 |
| 17 | Hounslow 2 – Cranford | 77 | 22/02 | 20 | 88 | 26 |
| 18 | Islington 1 – Upper Street | 72 | 08/08 | 25 | 91 | 27 |
| 19 | Kensington and Chelsea 1 – North Kensington | 77 | 08/08 | 29 | 90 | 29 |
| 20 | Mole Valley 2 – Lower Ashstead | 73 | 20/04 | 14 | 91 | 25 |
| 21 | Richmond 2 – Barnes Wetlands | 86 | 16/04 | 33 | 90 | 27 |

| Number | Name | Max daily mean TEOM* 1.3 (µg $m^{-3}$) | Date of max daily mean | Days >50 µg $m^{-3}$ | Data capture (%) | Annual mean TEOM* 1.3 (µg $m^{-3}$) |
|---|---|---|---|---|---|---|
| 22 | Southwark 1 – Elephant and Castle | 81 | 15/04 | 31 | 91 | 30 |
| 23 | Tower Hamlets 1 – Poplar | 168 | 15/04 | 42 | 88 | 31 |
| 24 | Tower Hamlets 3 – Bethnal Green | 72 | 10/08 | 28 | 85 | 27 |
| 25 | Waltham Forest 1 Dawlish Road | 66 | 20/04 | 16 | 69 | 25 |

**567.** Figure 6.42 shows the predicted distribution of annual mean $PM_{10}$ concentrations in 2003. The overall root mean square (RMS) error for the predicted data was 2.2 µg $m^{-3}$, and an assessment of predicted against monitored data showed that there is a tendency for lower concentrations to be overpredicted and higher concentrations to be underpredicted. There were no background locations estimated to exceed an annual mean of 30 µg $m^{-3}$ and also no locations with an estimated annual mean less than 23 µg $m^{-3}$.

**568.** As might be expected, Figure 6.42 shows a broad pattern of relatively high background concentrations through the centre of the city. It also suggests that there is a tendency for higher concentrations to occur towards the east of the city and lower concentrations towards the northwest and south. It should be noted that the limited number of background stations to the south of the conurbation may give additional uncertainty to the results presented here. Although the highest concentrations were estimated to occur in the northeast, this area is associated with relatively large error estimates (Figure 6.43).

**569.** Figure 6.44 shows estimated background annual mean $PM_{10}$ concentrations for 2002. Here the annual mean concentrations are generally lower, with a lower RMS error of 1.5 µg $m^{-3}$. In 2002, there were no background locations estimated to exceed 28 µg $m^{-3}$ and a number of areas to the south were estimated to be lower than 23 µg $m^{-3}$. It should be noted that the areas estimated to have a background concentration of 23 µg $m^{-3}$ or lower tended to be associated with a relatively high degree of uncertainty (standard errors were ~1.5–2.0 µg $m^{-3}$ (Figure 6.45)).

**570.** The results from both years show a similar pattern of background concentrations across London. The associated error maps are also broadly comparable and suggest that any additions to the existing network of background stations may be most beneficial in the south and northeast of the conurbation. The use of basic interpolation routines and background data, as in this example, would always tend to produce a more generalised map compared to the output of dispersion models that use emissions inventory data. The east-west gradient in concentrations suggested by the interpolated surfaces is not reflected in the maps produced from more detailed modelling studies (see Chapter 8). Since dispersion modelling of detailed emissions inventory data is the most reliable means of estimating the spatial distribution of annual mean $PM_{10}$ concentrations,

**Figure 6.42** Annual mean $PM_{10}$ concentrations across London in 2003 interpolated from background sites. (The number of days with a daily mean >50 µg $m^{-3}$ is also given for sites included in the study.)

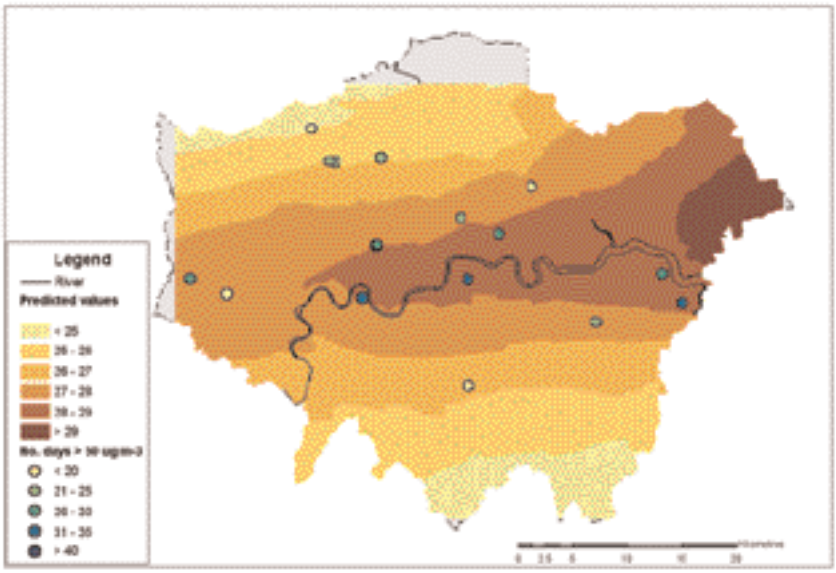


**Figure 6.43** Error estimates associated with predicted $PM_{10}$ annual average concentrations for 2003. (Predicted contours are shown for reference.)

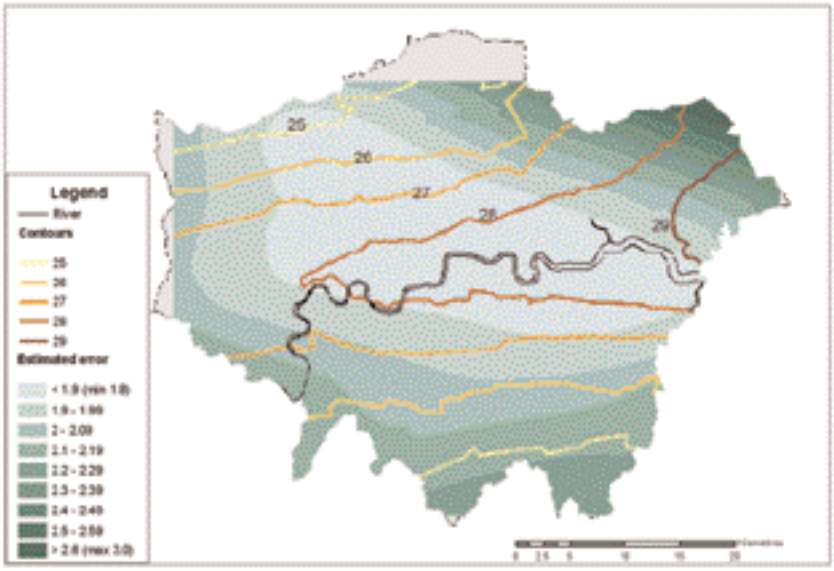


Figures 6.42 and 6.44 should be treated with caution. Rather than the maps reflecting true geographic variability, observed patterns from the interpolated surfaces could be associated with data artefacts linked to the specific siting characteristics of the stations shown in Table 6.1. These might include differences in the nature of local sources and their relative proximity to individual sites. More sophisticated interpolation-based approaches would be required to remove some of these uncertainties.

**571.** Maps generated from a dataset including both ß-attenuation monitor and TEOM monitoring stations are not reproduced in this section due to the uncertainty in generating comparable annual means. Following the application of the 1.3 scaling factor to TEOM sites, the highest concentrations were still clearly associated with

**Figure 6.44** Annual mean $PM_{10}$ background concentrations across London in 2002 interpolated from background sites. (The number of days with a daily mean >50 µg $m^{-3}$ is also given for sites included in the study.)

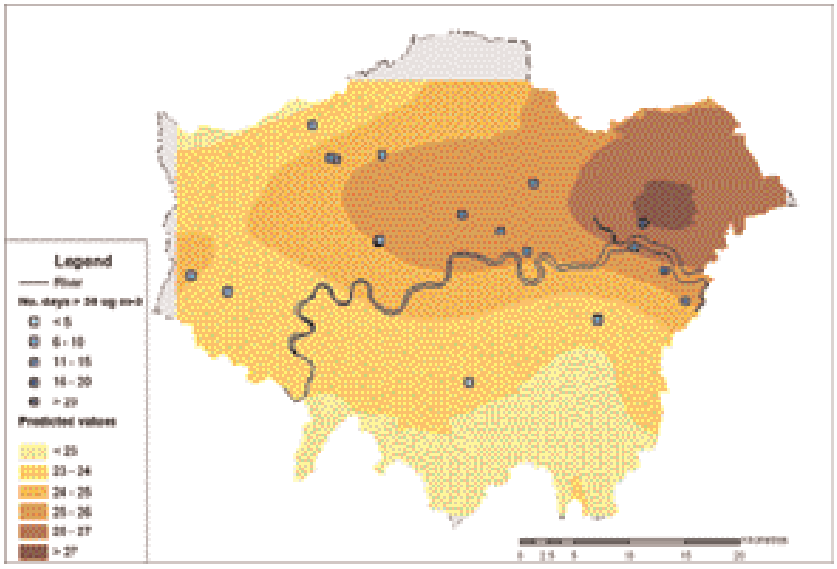


**Figure 6.45** Error estimates associated with predicted $PM_{10}$ annual average concentrations for 2002. (Predicted contours are shown for reference.)

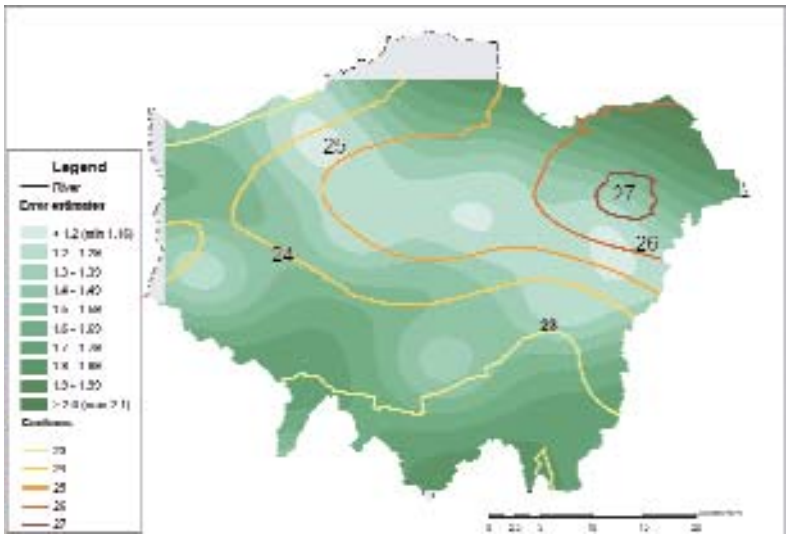


ß-attenuation monitor sites. The top three annual mean concentrations for 2003 were 35 µg $m^{-3}$ (Haringey 2 Priory Park), 36 µg $m^{-3}$ (Redbridge 1 Perth Terrace) and 38 µg $m^{-3}$ (Lambeth 3 Loughborough Junction) – considerably larger than the highest TEOM annual mean of 32 µg $m^{-3}$ (Barking and Dagenham 2 – Scrattons Farm). This issue is discussed further in Annex 4.

### 6.2.3.2 *Spatial distributions of $PM_{10}$ in London under episode conditions*

**572.** Surfaces showing the spatial distribution of concentrations associated with two particular episodes (labelled A and D on Figure 6.46), which occurred in London during 2003, have also been produced. Episode A occurred during the period 17th to 23rd February and was characterised by a high secondary particulate contribution from continental sources but with an important primary component.

Episode D was especially dominated by secondary particulate from continental sources and was a period of very high temperatures and photochemical activity that led to elevated ozone concentrations (Fuller, 2003). (See Chapter 8 for further discussion of the episode.)

**573.** Unscaled hourly concentration data were provided for 33 TEOM sites from the London and Southeast air quality networks and used to generate scaled 24-h means for the periods of interest. The data for February have been ratified but the data for August are a mix of ratified and non-ratified data. Due to incomplete data, not all of the sites may be included in each of the surfaces produced.

**574.** Figure 6.47 shows that during the February episode, the highest concentrations tended to be localized to the urban area of Greater London, with relatively high concentrations also estimated for North Kent. For some of the days, for example the 19th and 21st, there was also some evidence of relatively high concentrations on the southern coast, although there was a higher degree of error for these areas due to estimates being based on few data points (Figure 6.48).

**575.** The spatial pattern of the August episode (Figure 6.49 upper) appears to have had a wider impact over the entire Southeast region. Many of the surfaces show less variability in the error estimates than was the case for the February episode (Figure 6.49 lower). Although there is still some evidence of a distinct London effect, there are very high values estimated for the area north of the city (on 8th and 10th) and towards the south coast (on 11th).

**Figure 6.46** Daily mean $PM_{10}$ monitored at a typical London background site Kensington and Chelsea 1 – in 2003 (Fuller, 2003).

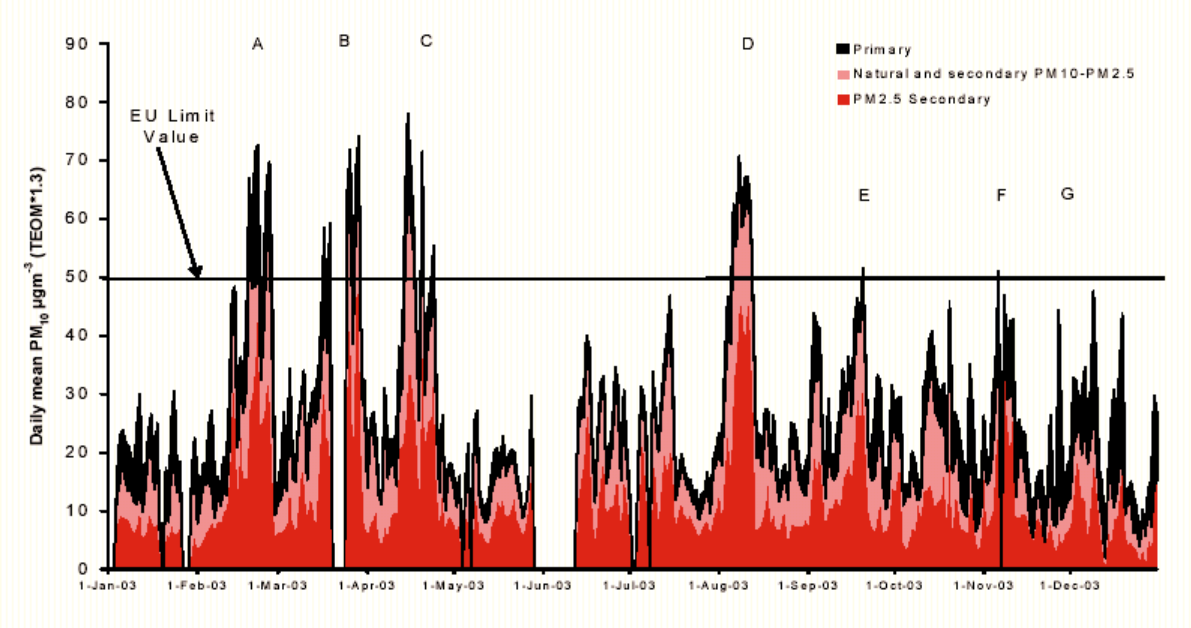

**Figure 6.47** Estimated spatial distributions of daily mean concentrations of $PM_{10}$ during 18th to 23rd February 2003.

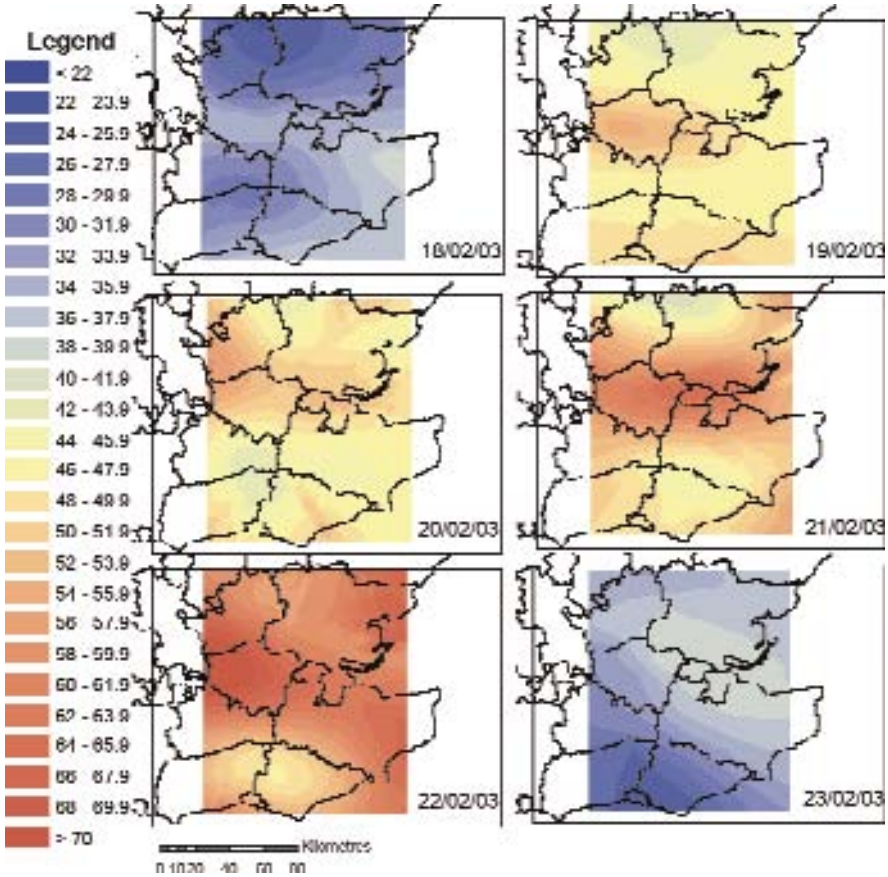


**Figure 6.48** Estimated spatial distribution of prediction errors during 18th to 23rd February 2003 (μg $m^{-3}$).

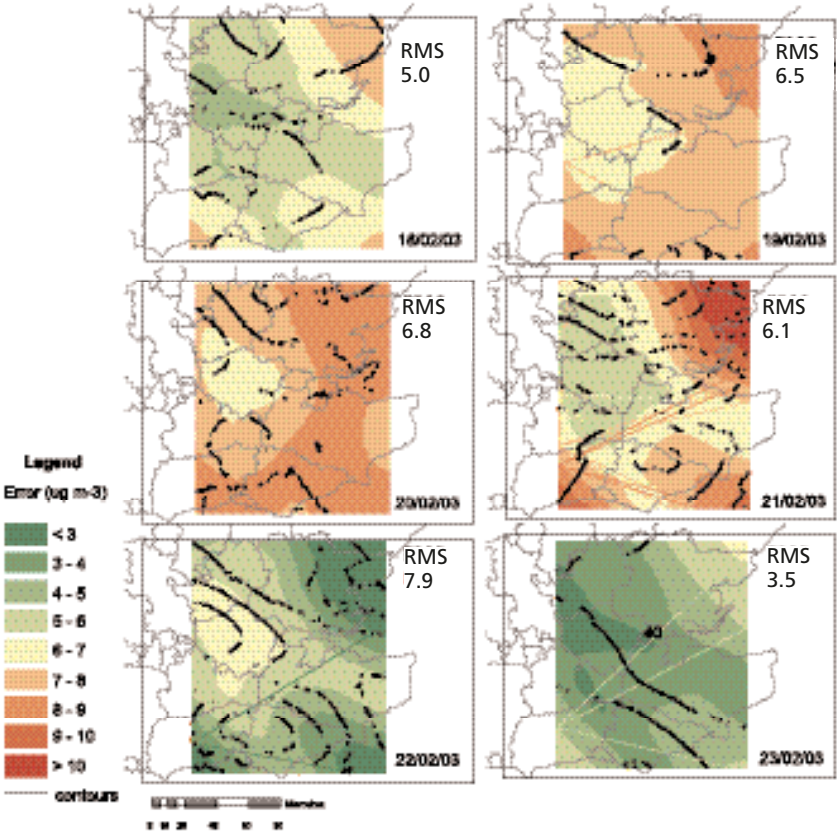

**Figure 6.49** (a) and (b) Estimated spatial distributions of daily mean concentrations of $PM_{10}$ during 7th to 15th August 2003 (μg $m^{-3}$).

(a)

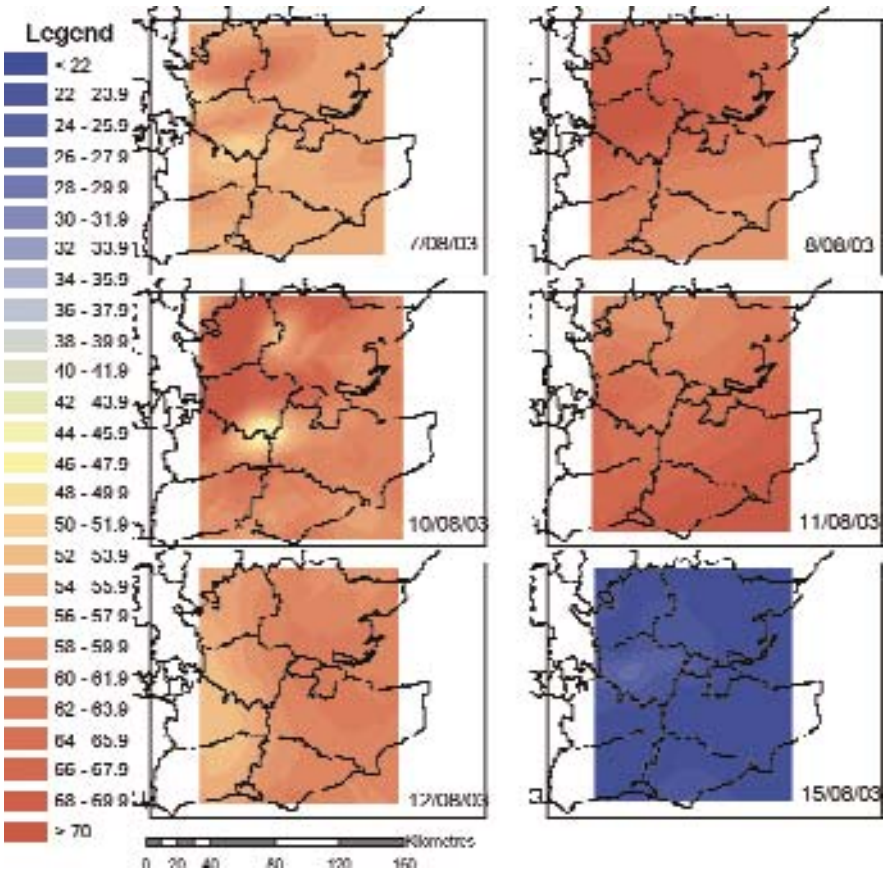


(b)

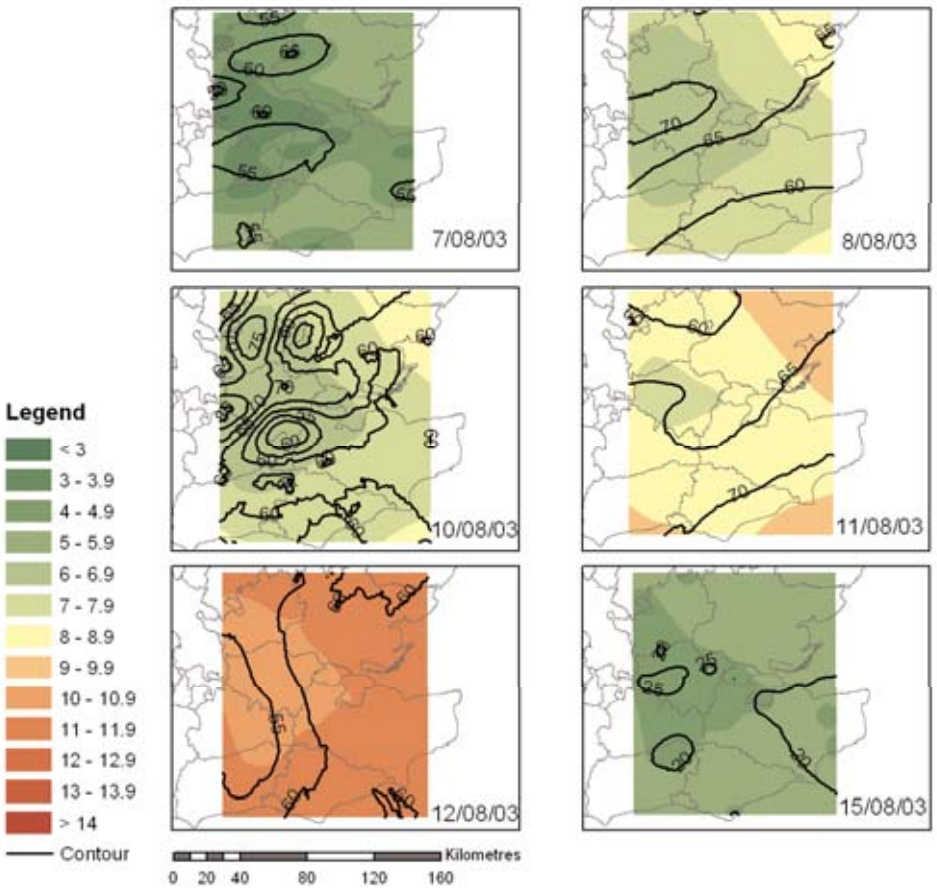

### 6.2.4 Roadside concentration distribution

**576.** The spatial variation of $PM_{10}$ concentrations alongside roads has not been studied in great detail. Only one study has been identified that shows the way in which concentrations decline away from roads. This study involved the use of MiniVol samplers alongside the M25 west of London (Hickman *et al.*, 2002). (REF to be supplied to list) These are gravimetric samplers that were used to collect daily samples for a total of 28 days split between November 1998 and March 1999. Comparison of the results with a TEOM sampler at the same location showed good agreement with TEOM * 1.3 values. Concentrations were measured on a transect both east and west of the motorway. The combined results for both transects, normalised to 100% at ~20 m from the edge of the carriageway, are illustrated in Figure 6.50. There is only evidence of a significant increase above the background within about 30 m of the carriageway. Beyond 20–50 m from the edge of the road, concentrations will be essentially indistinguishable from the local background, taking account of measurement uncertainty and the normally high background contribution to measured roadside concentrations.

**Figure 6.50** $PM_{10}$ gravimetric concentrations measured on transects away from the M25 motorway, normalised to 100% at ~20 m from the edge of the carriageway. (The data points have been fitted using a logarithmic relationship.)

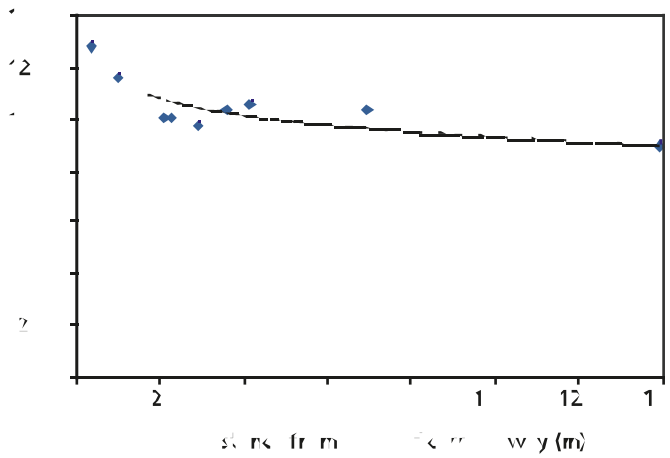


**577.** An additional survey was carried out to the west of the M25 motorway for 14 days in September 2000. On this occasion measurements were also made of $PM_{2.5}$. The ratios of $PM_{2.5}$:$PM_{10}$ ranged from 0.63 to 0.81, averaging 0.71,

**Figure 6.51** $PM_{10}$, $PM_{2.5}$ and $PM_{coarse}$ (gravimetric) concentrations measured on a transect away from the M25 motorway, normalised to 100% at ~20 m from the edge of the carriageway. (The line is the best-fit relationship from Figure 6.50.)

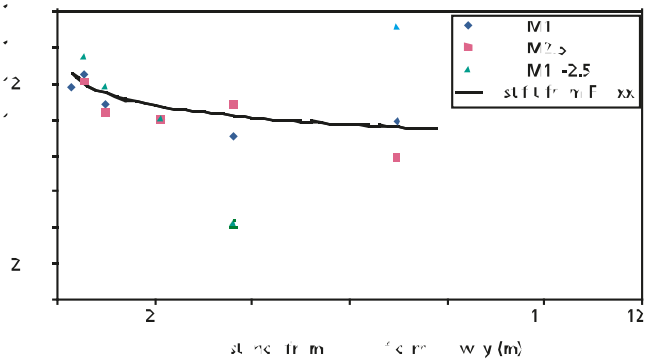

showing no systematic trend with distance. The results normalised to 100% at ~20 m from the edge of the carriageway are presented in Figure 6.51. Values for $PM_{coarse}$, calculated by difference, are also shown. The values in this figure are for the 10 days during which full datasets were available. Also shown in Figure 6.51 is the best-fit line taken from the earlier period, when more data were available (that is, from Figure 6.50). The same general pattern is seen as for the 1998–1999 monitoring, except that $PM_{coarse}$ is a much noisier signal.

### 6.2.5 Roadside increments of $PM_{10}$, $PM_{2.5}$ and $PM_{coarse}$

**578.** As part of the TRAMAQ study, Partisol Plus model 2025 dichotomous manual gravimetric samplers were used to collect simultaneous roadside and background samples at four different locations – Elephant and Castle, High Holborn and Park Lane in London and Selly Oak in Birmingham – with instruments being moved from site to site over a number of cycles to capture samples over all four seasons. The roadside sites were chosen on the kerbside of heavily trafficked roads, and the background sites were within 1 km of the roadside sites but at least 200 m from any busy road. The masses of the samples collected were determined in both fine ($PM_{2.5}$) and coarse ($PM_{2.5–10}$) fractions, and the $PM_{10}$ mass was calculated from the masses of the two fractions. Fuller details of the sites and measurements are given in Harrison *et al*. (2004).

**Table 6.11** The means (and standard errors) of the roadside, background and difference measurements of $PM_{10}$, $PM_{coarse}$ and $PM_{2.5}$ measured at each location. (Units are gravimetric μg $m^{-3}$.)

| | Roadside | | | Background | | | Difference | | |
|---|---|---|---|---|---|---|---|---|---|
| | **$PM_{10}$** | **$PM_{coarse}$** | **$PM_{2.5}$** | **$PM_{10}$** | **$PM_{coarse}$** | **$PM_{2.5}$** | **$PM_{10}$** | **$PM_{coarse}$** | **$PM_{2.5}$** |
| Elephant and Castle | 36.8 (3.6) | 12.5 (0.9) | 24.2 (2.9) | 21.2 (1.9) | 8.2 (0.5) | 13.0 (1.6) | 15.6 (2.0) | 4.4 (0.6) | 11.2 (1.4) |
| High Holborn | 38.3 (1.9) | 12.3 (0.7) | 25.9 (1.6) | 28.7 (1.9) | 10.8 (0.6) | 17.9 (1.6) | 9.6 (0.6) | 1.5 (0.4) | 8.0 (0.3) |
| Park Lane (EW) | 63.3 (3.9) | 21.3 (1.6) | 42.0 (3.7) | 27.9 (3.6) | 9.3 (0.9) | 18.6 (3.5) | 35.3 (1.3) | 12.1 (0.9) | 23.3 (1.2) |
| Park Lane (WW) | 22.8 (2.0) | 8.2 (0.6) | 14.6 (1.6) | 15.7 (1.3) | 5.7 (0.4) | 10.0 (1.1) | 7.1 (0.9) | 2.5 (0.3) | 4.6 (0.6) |
| Selly Oak | 25.1 (1.2) | 9.1 (0.4) | 16.0 (0.9) | 16.4 (1.0) | 7.0 (0.3) | 9.4 (0.7) | 8.7 (0.4) | 2.1 (0.2) | 6.6 (0.3) |

**579.** The mean values of $PM_{10}$, $PM_{coarse}$ and $PM_{2.5}$ measured at the roadside and background sites at each of the four locations are presented in Table 6.11. The means of the differences between the individual measurements at the roadside and background sites are also shown. Due to the wide variation in the differences for the Park Lane data, it is separated into two groups: easterly winds (EW), when the wind direction was between 0° and 180° and westerly winds (WW). Wind data were obtained from Heathrow Airport.

**580.** The roadside concentrations of $PM_{10}$, $PM_{coarse}$ and $PM_{2.5}$ are plotted against their respective values at background sites for each of the four locations in Figures 6.52 to 6.55. Lines are fitted by the reduced major axis (RMA) regression due to the similar uncertainty in the values of concentration at both the roadside and background sites (Ayers, 2001). The equations for the lines and values of the squared correlation coefficient are given in Table 6.12.

**Table 6.12** Results of regression analysis of roadside ($y$) versus background ($x$) concentrations.

| Location | | RMA regression | $r^2$ |
|---|---|---|---|
| Elephant and Castle | $PM_{10}$ | $y = 1.94\ x - 4.32$ | 0.88 |
| | $PM_{coarse}$ | $y = 1.79\ x - 2.14$ | 0.57 |
| | $PM_{2.5}$ | $y = 1.81\ x + 0.65$ | 0.91 |
| High Holborn | $PM_{10}$ | $y = 1.03\ x + 8.78$ | 0.90 |
| | $PM_{coarse}$ | $y = 1.27\ x - 1.33$ | 0.62 |
| | $PM_{2.5}$ | $y = 1.00\ x + 8.07$ | 0.96 |
| Park Lane (EW) | $PM_{10}$ | $y = 1.10\ x + 32.57$ | 0.90 |
| | $PM_{coarse}$ | $y = 1.79\ x + 4.72$ | 0.86 |
| | $PM_{2.5}$ | $y = 1.07\ x + 22.07$ | 0.90 |
| Park Lane (WW) | $PM_{10}$ | $y = 1.55\ x - 1.52$ | 0.91 |
| | $PM_{coarse}$ | $y = 1.45\ x - 0.07$ | 0.75 |
| | $PM_{2.5}$ | $y = 1.39\ x + 0.63$ | 0.91 |
| Selly Oak | $PM_{10}$ | $y = 1.24\ x + 4.70$ | 0.88 |
| | $PM_{coarse}$ | $y = 1.15\ x + 1.05$ | 0.76 |
| | $PM_{2.5}$ | $y = 1.31\ x + 3.68$ | 0.90 |

**581.** It is notable that for High Holborn the regression lines for $PM_{10}$ and $PM_{2.5}$ have a smaller gradient (approximately 1:1) and larger intercept than is the case for Elephant and Castle or Selly Oak. The constant increment of $PM_{10}$ and $PM_{2.5}$ at all background concentrations at High Holborn indicates that the increment at this location is not determined by the factors that influence the level of the background concentrations. The High Holborn sites are within central London street canyons with building heights greater than the cross street distance between buildings. The Elephant and Castle and Selly Oak sites are considerably more open and meteorological factors are much more likely to affect particulate matter concentrations.

**582.** At Park Lane the nature of the regression depended upon the wind direction. In easterly winds the gradients of the $PM_{10}$ and $PM_{2.5}$ regression equations are close to unity and the intercepts are large and positive, similar to the results obtained at High Holborn. In westerly winds the results at Park Lane are similar to those seen at the Elephant and Castle and Selly Oak locations. The Park Lane roadside site is on the eastern side of the road with a substantial building (The Intercontinental Hotel) at the rear of the footway. On the opposite side of the road is Hyde Park and an absence of buildings. During easterly winds

it might be expected that a wind flow regime similar to that experienced in a street canyon would occur with winds passing over the top of the building and establishing a rotating flow in the lee of the building giving rise to the higher concentrations seen in Table 6.11, as the reverse flow brings PM from the direction of the road. No such rotating flow would be seen during westerly winds. While making these comparisons it should be noted that the number of measurements made during easterly winds at Park Lane was small (nine) and that the results are heavily influenced by individual measurements.

**583.** The effects of wind speed on $PM_{10}$ concentrations at Park Lane are shown in Figure 6.56. In westerly winds there is a general decrease in concentration with wind speed, consistent with greater dilution of PM occurring in higher wind speeds. In easterly winds $PM_{10}$ tends to increase with higher wind speeds, presumably as the rotor effects become stronger and the reverse flow draws more air onto the instruments from the roadway.

**Figure 6.52** Elephant and Castle – roadside concentration versus background concentration.

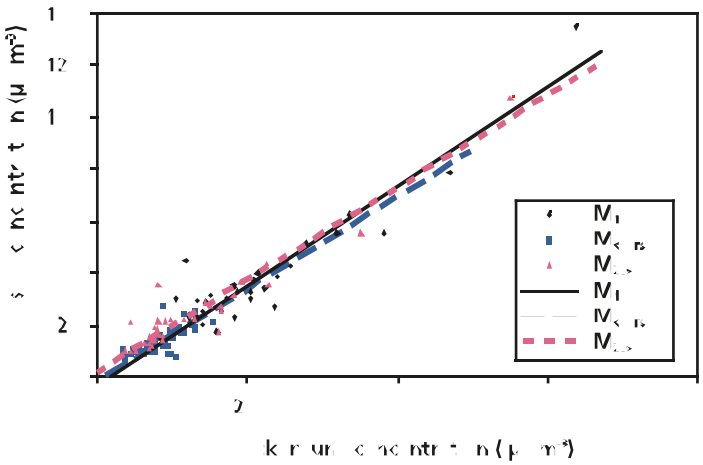

**Figure 6.53** High Holborn – roadside concentration versus background concentration.

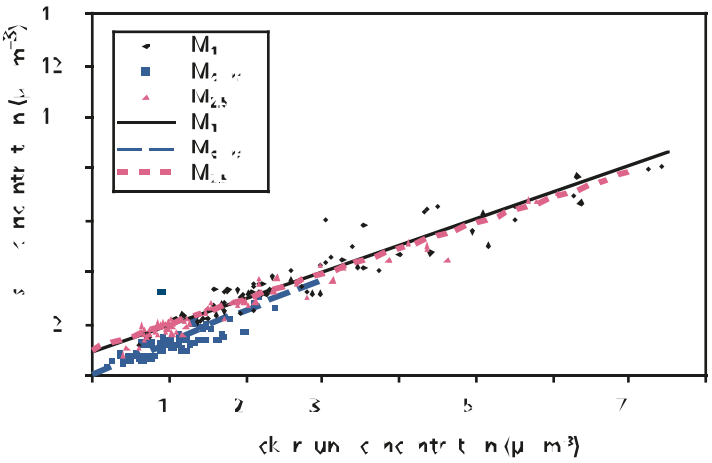

**Figure 6.54** Park Lane – roadside concentration versus background concentration.

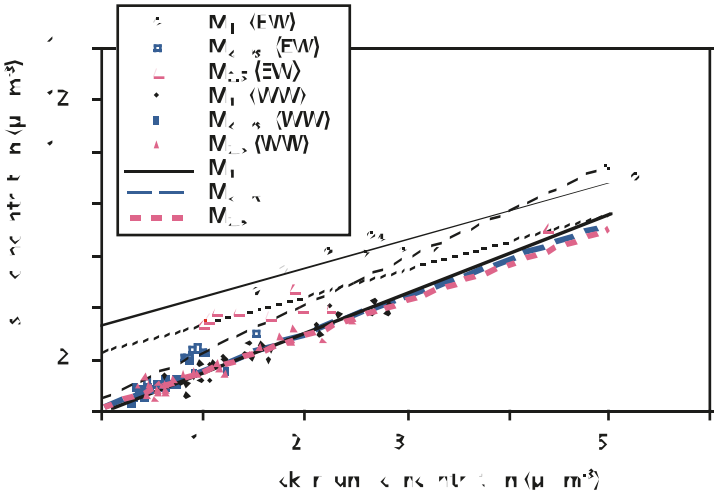

**Figure 6.55** Selly Oak – roadside concentration versus background concentration.

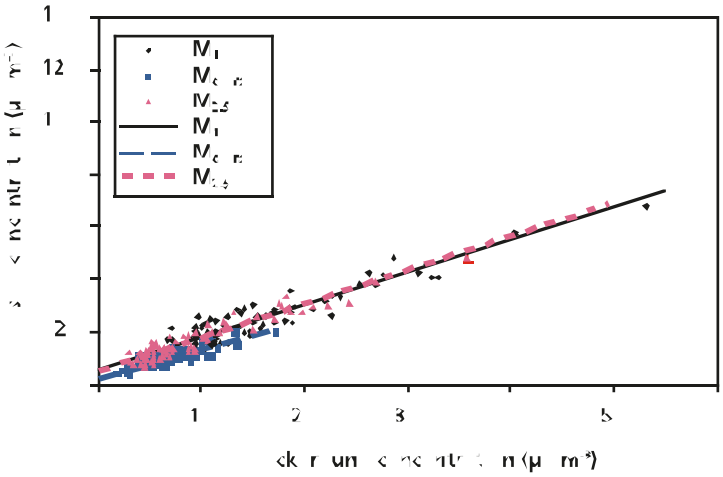

**Figure 6.56** Park Lane – effect of windspeed on $PM_{10}$ increment.

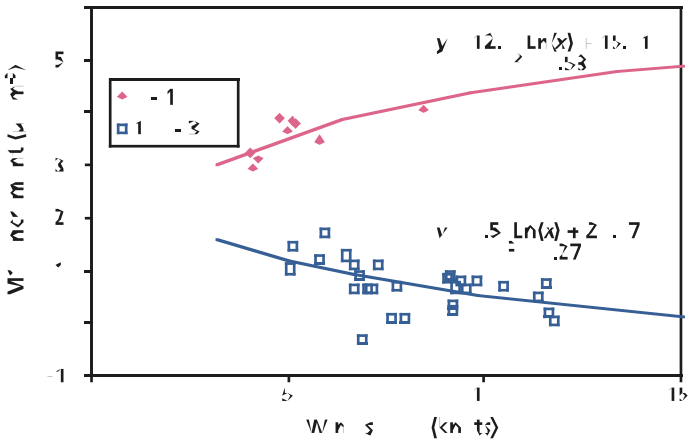

## 6.2.6 Spatial distribution of secondary constituents across the UK

**584.** Maps of sulphate, nitrate and ammonium (Figures 6.57 to 6.59) have been derived from measurements made by the Centre for Ecology and Hydrology (CEH). The sulphate and nitrate maps have been interpolated from monthly

measurements at a network of 12 rural sites. The sulphate and nitrate maps have a southeast to northwest gradient. Ammonium shows similar gradients to those seen for nitrate.

**Figure 6.57** Annual mean sulphate concentration (μg $m^{-3}$) for 2002.

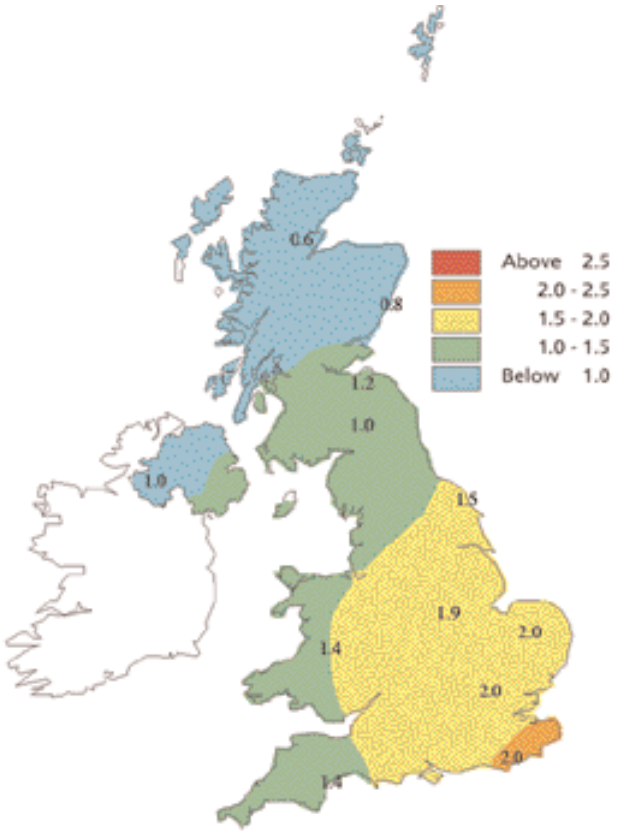


**Figure 6.58** Annual mean nitrate concentration (μg $m^{-3}$) for 2002.

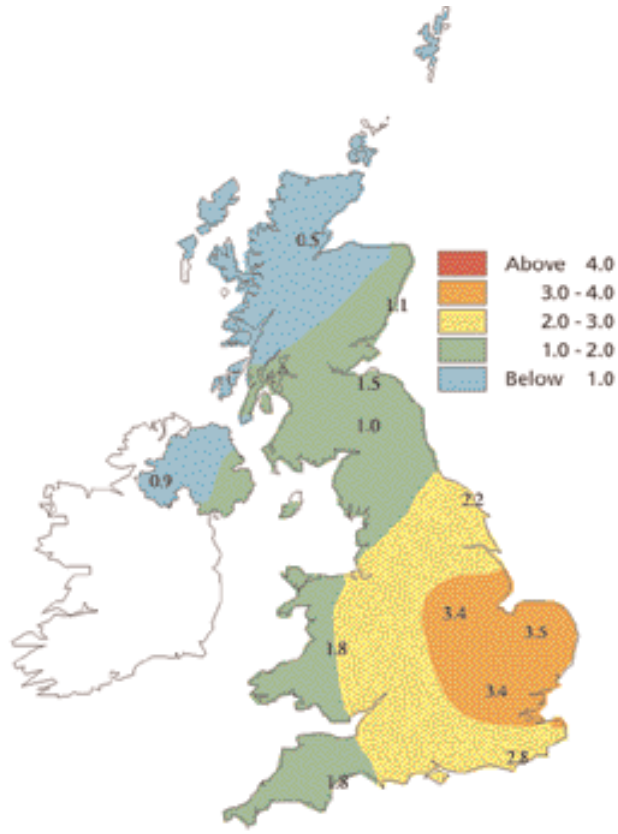

**Figure 6.59** Annual mean ammonium concentration (μg $m^{-3}$) for 2002.

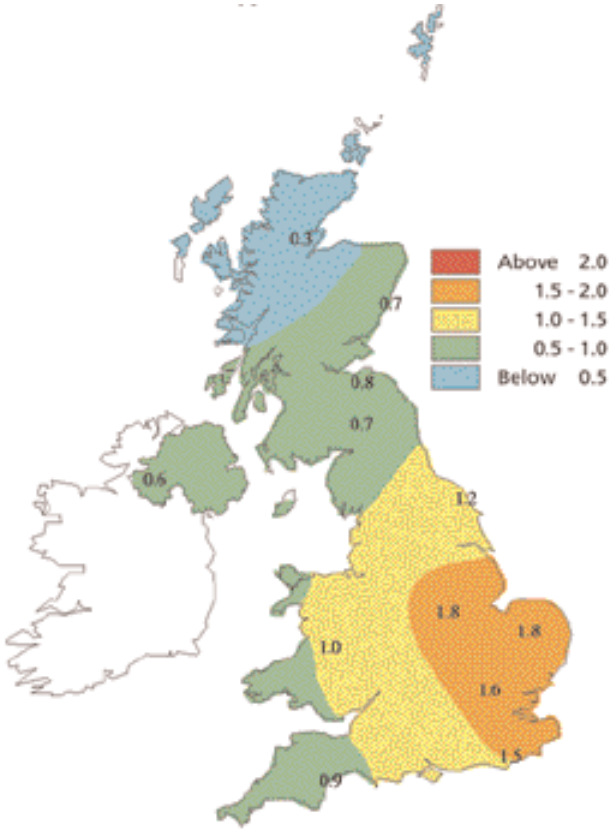


**Figure 6.60** Annual mean chloride concentration (μg $m^{-3}$) for 2002.

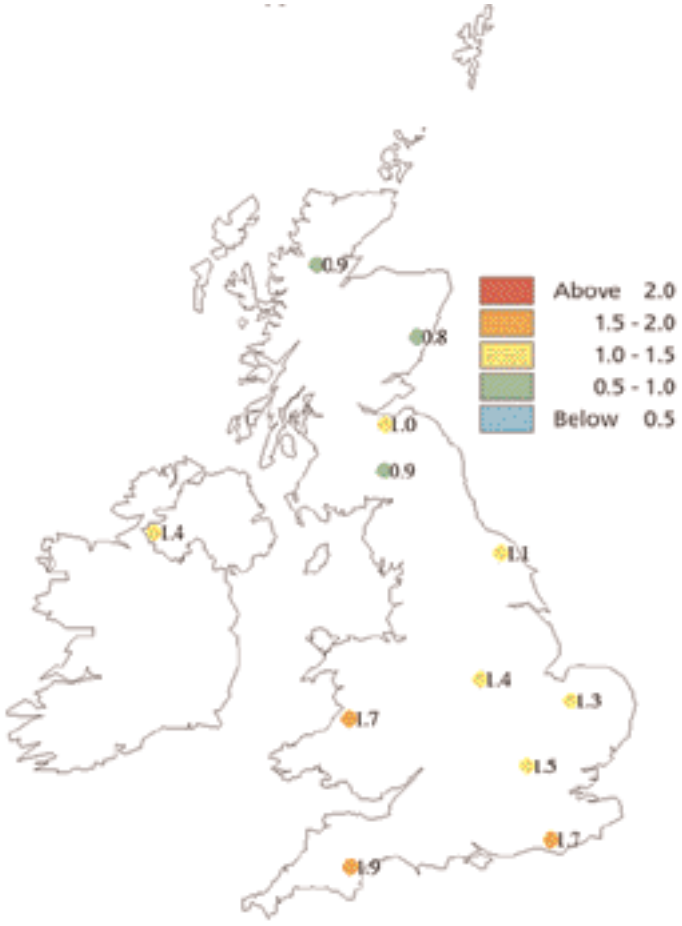

**585.** Chloride concentrations have also been measured at these sites. Chloride concentrations have more small-scale spatial variation than the secondary sulphate and nitrate concentrations. In particular the 12-site network does not provide enough information on the gradients in chloride concentrations close to the coast. The spatial pattern of chloride concentrations is also more variable from year to year. Chloride concentrations have, therefore, not been interpolated in Figure 6.60. In 2002 there are indications of a southwest to northeast gradient.

## 6.3 Episodicity of particle concentrations

### 6.3.1 Monthly exceedences of air quality objective concentrations

**586.** Figure 6.61 shows the number of exceedences of 50 µg $m^{-3}$ (TEOM * 1.3) measured each month between January 1996 and December 2003 at national network sites. There was an increase in the number of monitoring sites over this period, so the number of sites operational during each year is also shown. The total number of measured exceedences tended to increase as the number of sites in the network increased, since an exceedence can occur at several sites on the same day. Figure 6.61 shows the number of monthly exceedences divided by the number of operational sites in each year. This should provide an estimate of the number of exceedences that is reasonably independent of the number of sites.

**Figure 6.61** Number of daily $PM_{10}$ AQS exceedences summed across AURN by month (1996–2003).

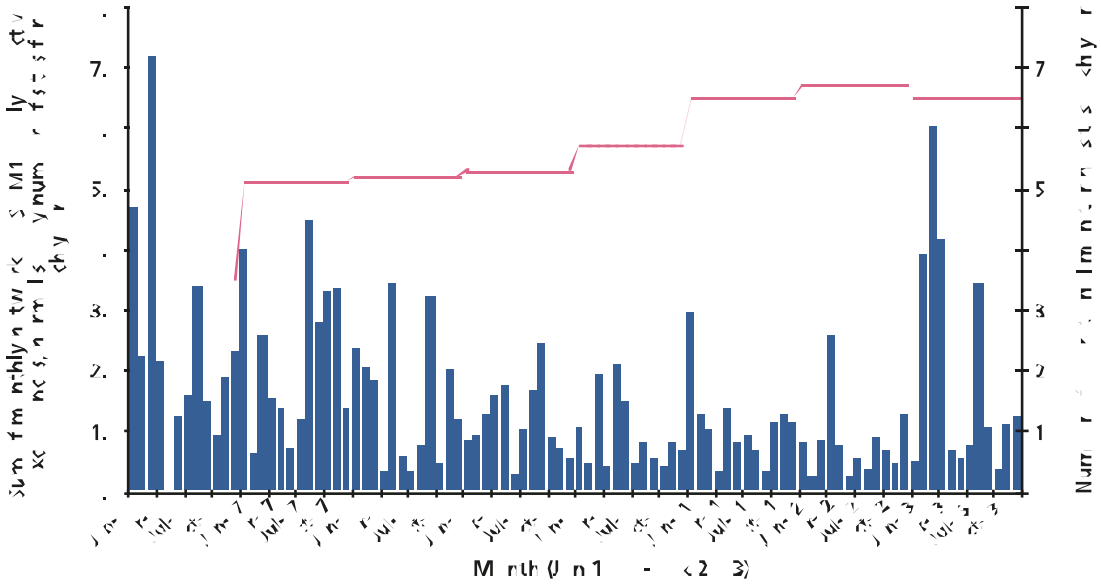


**587.** Figure 6.61 shows that there is a considerable month-to-month variation in the number of exceedences. The number of exceedences has generally declined since 1996 but the number of exceedences during 2003 was unusually high. The episodes seen in Figure 6.61 had a range of causes. There were notable winter secondary PM episodes in January and March 1996 and in early 2003. The photochemical episode that happened in August 2003 is also clearly shown. Episodes were also caused by poor dispersion of primary pollutants, such as during the autumn of 1997. Long range transport dust events such as those that occurred in March 2000 and early 2003 are also shown.